energies

Article

Energy Scheduling Strategy for the Gas–Steam–Power System in Steel Enterprises Under the Influence of Time-Of-Use Tariff

Jun Yan [1], Yuqi Zhao [2], Qianpeng Hao [1], Yu Ji [2], Minhao Zhang [1], Huan Ma [2] and Nan Meng [2,*]

[1] Inner Mongolia Power (Group) Co., Ltd., Hohhot 010010, China; 15922153310@163.com (J.Y.); 15184764613@163.com (Q.H.); zhangminhao@impc.com (M.Z.)
[2] Key Laboratory for Thermal Science and Power Engineering of Ministry of Education, Department of Engineering Mechanics, Tsinghua University, Beijing 100084, China; 13352348338@163.com (Y.Z.); jysquanchy@163.com (Y.J.); mahuan@mail.tsinghua.edu.cn (H.M.)
* Correspondence: ccmn0909@163.com

Abstract: Fully harnessing the inherent flexible adjustment potential of steel enterprises and fostering their interaction with the power grid is a crucial pathway to advancing green transformation. However, traditional research usually takes reducing energy consumption as the optimization goal, which limits the adjustment response capability, or ignores the storage and conversion constraints of secondary energy sources such as gas, steam, and electricity, making it difficult to fully explore and reasonably utilize the potential of multi-energy coordination. This study considers the production constraints of the surplus energy recovery and utilization system, establishes a collaborative scheduling model for a gas–steam–power system (GSPS) in an iron and steel enterprise, and proposes a demand response strategy that considers internal production constraints. Considering the time-of-use (TOU) tariff, iron and steel enterprises achieve a dynamic optimization adjustment range of electricity demand response through the conversion and storage process of gas, steam, and power. The adjustment capability of the GSPS reaches 26.94% of the initial electricity load, while reducing the total system energy cost by 2.24%. There is vast development potential of iron and steel enterprises participating in electricity demand response for promoting cost reduction and efficiency improvement, as well as enhancing the power grid flexibility.

Keywords: demand response; gas–steam–power system; optimize scheduling; steel production; TOU tariff

Academic Editor: Seung-Hoon Yoo

Received: 8 January 2025
Revised: 20 January 2025
Accepted: 24 January 2025
Published: 4 February 2025

Citation: Yan, J.; Zhao, Y.; Hao, Q.; Ji, Y.; Zhang, M.; Ma, H.; Meng, N. Energy Scheduling Strategy for the Gas–Steam–Power System in Steel Enterprises Under the Influence of Time-Of-Use Tariff. *Energies* **2025**, *18*, 721. https://doi.org/10.3390/en18030721

1. Introduction

The steel industry plays a foundational role in the global economy, supporting key sectors such as construction, manufacturing, and transportation. At the same time, it has a significant impact on energy consumption and carbon emissions. According to data from 2022, five major energy-intensive industries, including steel and non-ferrous metal smelting, account for 45% of China's total energy consumption [1], with the steel industry alone contributing 14% of energy consumption [2] and 15.9% of carbon emissions [3]. This substantial environmental footprint makes the steel industry a critical area for achieving China's "dual carbon" goals, highlighting the urgent need for energy-saving, emission-reduction, and industrial transformation [4], and further emphasizing the industry's central role in future sustainable development [5]. Reducing energy consumption and carbon emissions while maintaining production efficiency and quality is one of the most pressing challenges facing the steel industry [6]. Studies have pointed out that during the industry's transformation, a balance must be struck between environmental goals and production capacity [7].

Although steel production relies heavily on fossil fuels such as coal and natural gas, it also generates significant amounts of secondary energy, such as gas, steam, and electricity [8]. However, traditionally, these by-products have not been effectively recovered or utilized in steel production [9]. Research indicates that the recovery and reuse of secondary energy is key to improving overall energy efficiency in the steel industry [10]. Moreover, using these by-products can reduce dependence on external energy sources [11] and significantly enhance self-sufficiency in energy [12]. By strategically allocating and dynamically scheduling these energies, steel enterprises can enhance their self-generation capacity [13], reduce the burden on the power grid [14], and increase the grid's ability to integrate renewable energy [15].

With the growing maturity of demand response (DR) mechanisms, steel enterprises, as flexible load resources, can adjust their energy consumption to support the grid during peak demand periods [16]. This flexibility not only stabilizes the grid [17] but also facilitates the large-scale integration of renewable energy. Studies have shown that by optimizing the dynamic conversion, storage, and distribution of gas, steam, and electricity, steel enterprises can reduce their reliance on traditional fossil fuels without compromising production, thereby driving green transformation. These measures also contribute to achieving China's "dual carbon" goals, further pushing the industry toward sustainable development. As Yuan et al. have pointed out, methods for improving energy efficiency in steel production face multiple challenges, yet they also offer a variety of optimization pathways and promising prospects for future development [18].

In recent years, extensive research has focused on optimizing the allocation of secondary energy in steel production. Early studies concentrated on optimizing individual energy resources, such as gas [19,20], steam [21,22], and electricity [23,24]. Akimoto et al. [25] proposed a mixed-integer linear programming (MILP) model for optimizing gas resource allocation in steel enterprises, while Zhao et al. [26] developed an MILP model that includes penalty factors for boilers and gas storage to optimize gas distribution and reduce operational costs [27]. However, these studies generally focused on optimizing single energy types [28], overlooking the synergistic effects between gas, steam, and electricity and their impact on system flexibility [29].

Building on this, Shu et al. [30] introduced a collaborative scheduling model for gas, steam, and electricity, aimed at minimizing the overall operational cost by optimizing the integration of these energy types. While this model lays the theoretical groundwork for energy optimization, it still faces limitations, such as failing to account for dynamic changes in the supply and demand of gas, steam, and electricity, as well as production constraints like burner switching and gas storage safety. Therefore, a key challenge remains: how to optimize energy allocation while considering various production constraints.

To address these issues, He et al. [31] proposed a linear programming model that considers the dynamic variations in the demand for gas, steam, and electricity, along with the impacts of rolling schedules on energy dispatch [32]. Similarly, Zhao et al. [33] suggested an MILP model for optimizing secondary energy allocation in steel enterprises, based on time-of-use (TOU) electricity pricing and dynamic boiler efficiency. However, these studies largely overlook the collaborative role of critical internal energy systems, particularly the synergy between combined heat and power (CHP) units and waste heat recovery systems. As a result, these models have not fully enhanced system flexibility and efficiency.

In summary, the dynamic coordination and optimization of gas, steam, and electricity in steel enterprises is an effective approach to improving operational efficiency and enhancing system flexibility. While much of the existing research has made progress in optimizing individual energy types, it has not fully considered the coupling effects between different energy forms or properly accounted for the internal constraints of the production process. This limits the precise assessment and effective utilization of system flexibility. Moreover, most studies focus primarily on reducing operational costs under fixed electricity prices [34], neglecting the potential of steel enterprises to act as flexible load resources interacting with the grid [35].

To solve the above problems, this study selects a steel enterprise in Northeast China as a case study and first establishes an integrated gas–steam–electricity coupling optimization scheduling model. This model incorporates the internal production processes of the waste energy recovery system, focusing on the time-series coupling, conversion, and storage of gas, steam, and electricity. Based on this, the model considers production constraints such as the level changes in gas storage and boiler burner switching. Additionally, the study proposes a dynamic electricity demand response strategy based on peak, valley, and standard time periods, optimizing the electricity demand response strategy by leveraging the complementary characteristics of multi-energy conversion and the convenience of gas storage, thereby reducing dependence on external energy sources. Finally, this study quantitatively evaluates the load adjustment potential of the steel enterprise under different electricity price conditions and analyzes how the enterprise can provide flexible regulation to the grid through load response, thus promoting the green transformation of the steel enterprise and the stability of the power grid.

2. Problem Statement

A typical long flow steelmaking process includes sintering, pelletizing, coking, ironmaking, steelmaking, and hot rolling. During the coking process, washed coal is transformed into coke in coke ovens, and coke oven gas (COG) is recovered. Waste heat from the coke ovens is also captured through dry quenching (CDQ) technology, which generates electricity and steam. In the ironmaking process, raw materials such as sintered ore and coke are fed into the blast furnace to reduce iron ore to molten iron, and blast furnace gas (BFG) is recovered from the top of the blast furnace as a by-product. In the steel-making process, the carbon in the molten iron undergoes an oxidation reaction with oxygen to produce qualified molten steel, and the flue gas is recovered and purified to be converter gas (LDG) that can be used. In addition to the three types of gas in the production process to meet the needs of steel production, the surplus gas can be converted into steam, electricity and other energy sources to further meet the production needs. Figure 1 illustrates the main structure of the steel production process and the associated energy recovery and utilization system. COG and BFG are used to supply energy to the steam boilers (B1-B4) and the CHP unit, and are also utilized in the main process coke ovens for coke production and hot rolling. The high-pressure steam S1 (3.5 MPa), medium-pressure steam S2 (1.0 MPa), and low-pressure steam S3 (0.4 MPa) produced by the steam boilers are used in the main process. Additionally, high-pressure steam S1 drives steam turbines (TB1, TB2) for electricity generation. Steam S2, generated from the dry quenching power generation process, is also used in the main process. The steam turbine, CHP unit and CDQ unit together with the purchased power from the grid supply the production process.

In steel plants, boiler loads are regulated by controlling the burners, with most boilers being equipped with multiple burners to accommodate different types of by-product gas. To maintain safe boiler operation and avoid issues such as tempering or incomplete combustion, it is essential to minimize the frequent opening and closing of burners.

Additionally, gas cabinets act as a buffer between gas production and utilization, enabling gas storage for backup purposes, coordinating upstream and downstream production processes, and ensuring production safety. Different types of gas cabinets are limited by capacity constraints, and there are normal inventory levels and safe operating intervals. Taking the industrial production of an iron and steel plant in Northeast China as an example, the inventory levels of COG, BFG, and LDG in the gas cabinet should be kept near 100 km^3, 180 km^3, and 40 km^3, respectively, and can fluctuate within 80–120 km^3, 140–220 km^3, and 25–55 km^3. Once the gas cabinet reaches its maximum storage capacity, any excess by-product gas must be vented.

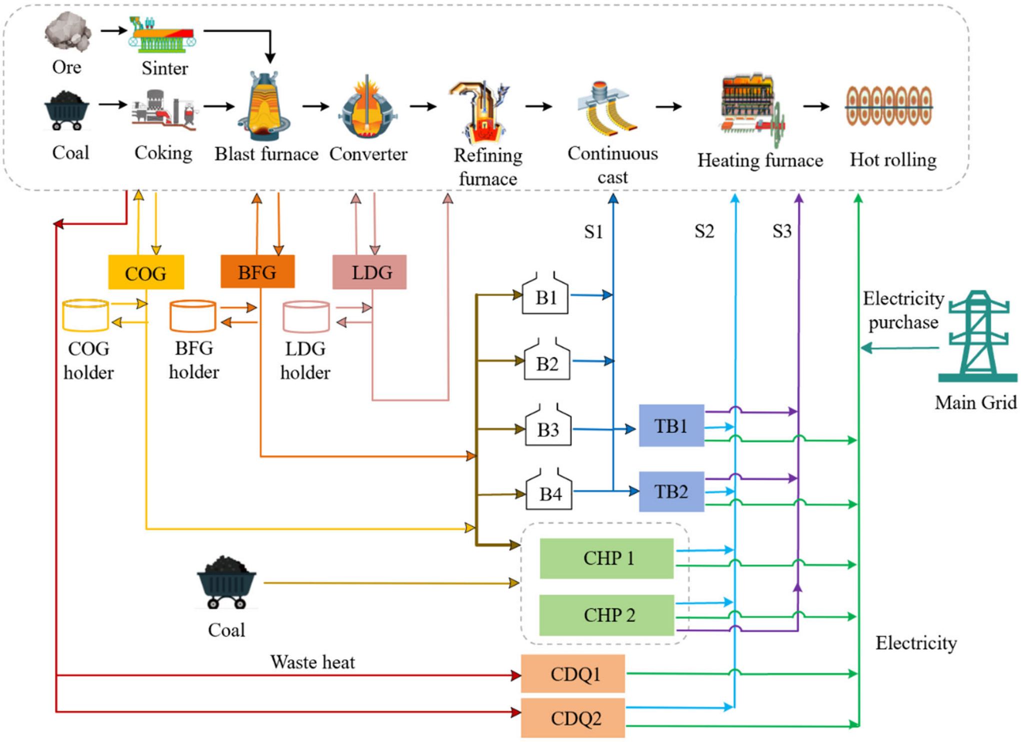

Figure 1. Diagram of the GSPS in the iron and steel enterprise.

3. Mathematical Model

This study aims to explore gas, coal, steam, and electricity distribution and dispatch in the iron and steel enterprise over a 24-h period (t = 1, 2, . . ., 24). Each period starts at H_{t-1} and ends at H_t, which gives

$$\tau_t = H_t - H_{t-1} \tag{1}$$

A. Steam and Power Generation Model

The by-product gas used as fuel in the boiler generates different temperature grates of steam, which is then applied in the main production process and waste heat power generation system. The steam and power generation model comprises steam boilers, turbines, CHP units, and CDQ units.

(1) Boilers

Boilers in steel enterprises are capable of consuming multiple types of by-product gases, such as COG and BFG, to produce steam of varying energy grades (S1, S2, and S3). The energy balance and constraint equations for steam boilers are [35]

$$\sum_{r=1}^{R} (S_{irt} \cdot h_r^s) - S_{it}^w \cdot h^w = \eta_i \left(\sum_{q=1}^{Q} V_{iqt} \right) \tag{2}$$

$$\sum_{q=1}^{Q} V_{iqt} \cdot hv_q \geq \left(\sum_{q=1}^{Q} V_{iqt} \right) \cdot hv_i^{\min} \tag{3}$$

$$S_{it}^{w} = \sum_r S_{irt} \tag{4}$$

$$0 \leq V_{iqt} \leq V_{iq}^{\max} \tag{5}$$

$$S_{ir}^{\min} \leq S_{irt} \leq S_{ir}^{max} \tag{6}$$

where r (r = 1, 2, . . ., R) represents the different grades of steam, i (i = 1, 2, . . ., I) represents the different boilers, and t represents time (t = 1, 2, . . ., 24). S_{irt} represents the flow rate of steam of grade r produced by boiler i during time period t, S_{it}^{w} represents the feedwater flow rate of boiler i during time period t. h^{s} *and* h^{w} represent the specific enthalpy of steam and feedwater, respectively. V_{iqt} represents the feed flow rate of fuel q supplied to boiler i during time period t. In boilers, q indicates BFG and COG. η_i represents the thermal efficiency of boiler i. hv_{q} is the calorific value of different gases, and $hv_i^{\min}$ is the minimum calorific value required for the normal operation of boiler i. Equation (4) ensures that the total amount of steam generated by a boiler equals its total feedwater input. $V_{iq}^{\max}$ indicates the maximum flow rate of the q type of fuel fed into the boiler. $S_{ir}^{\min}$ indicates the minimum flow rate of the r level steam generated from the boiler. $S_{ir}^{\max}$ indicates the maximum flow rate of the r level steam generated from the boiler.

Steam Turbines

The relationship between the inlet and outlet steam flows for the turbine during each time period can be expressed by [36]

$$S_{jt}^{\mathrm{in}} = S_{jt}^{out} \tag{7}$$

$$S_{jt}^{\mathrm{in}} = \sum_r S_{jrt}^{\mathrm{in}} \tag{8}$$

$$S_{jt}^{out} = \sum_r S_{jrt}^{out} \tag{9}$$

$$f_{jt} = \eta_i \cdot \left[\sum_r \left(S_{jrt}^{in} \cdot h_r^s \right) - \sum_r \left(S_{jrt}^{out} \cdot h_r^s \right) \right] \tag{10}$$

$$S_{jr}^{in,\min} \leq S_{jrt} \leq S_{jr}^{in,\max} \tag{11}$$

$$S_{jr}^{out,\min} \leq S_{jr} \leq S_{jr}^{out,\max} \tag{12}$$

$$f_j^{\min} \leq f_{jt} \leq f_j^{\max} \tag{13}$$

$$DR_j \leq f_{jt} - f_{jt-1} \leq UR_j \tag{14}$$

where j (j = 1, 2, . . ., J) represents different turbines. S_{jt}^{in} and S_{jt}^{out} denote the flow rate of steam into and out of the turbine j, respectively, during time period t. S_{jrt}^{in} and S_{jrt}^{out} represent the flow rate of grade r steam into and out of the turbine j, respectively, during time period t. $f_{j,t}$ denotes the power generation of turbine j during time period t and η_i represents the thermal efficiency of turbine i. $S_{jr}^{\mathrm{in,min}}$ and $S_{jr}^{\mathrm{in,max}}$ represent the minimum and maximum flow rate of the r level steam into the turbine, respectively. $S_{jr}^{\mathrm{out,min}}$ and $S_{jr}^{\mathrm{out,max}}$ represent the minimum and maximum flow rate of the r level steam out of the turbine, respectively. $f_j^{\min}$ and $f_j^{\max}$ represent the minimum and maximum electricity generation rate from the turbine, respectively. DR_j and UR_j represent the maximum ramp down and up rate of the turbine, respectively.

(2) CHP

CHP units commonly found in iron and steel enterprise generally comprise fuel boilers, steam turbines, and gas turbines. The input energy sources include gas and coal, and the output includes electricity and steam. The CHP model is as follows [37].

$$f_{kt} + \sum_{r=1}^{R} (S_{krt} \cdot h_r^s - S_{krt} \cdot h^w) = \eta_k \cdot \left[\sum_{i \in I_k} \sum_{q=1}^{Q} (V_{iqt} \cdot hv_q) \right] \tag{15}$$

$$\sum_{i \in I_k} \sum_{q=1}^{Q} (V_{iqt} \cdot hv_q) \geq hv_k^{\min} \cdot (\sum_{i \in I_k} \sum_{q=1}^{Q} V_{iqt}) \left(\sum_{i \in I_k} \sum_{q=1}^{Q} V_{iqt} \right) \tag{16}$$

$$0 \leq V_{iqt} \leq V_{iq}^{\max} \tag{17}$$

$$S_{kr}^{\min} \leq S_{krt} \leq S_{kr}^{\max} \tag{18}$$

$$f_k^{\min} \leq f_{kt} \leq f_k^{\max} \tag{19}$$

$$DR_k \leq f_{kt} - f_{kt-1} \leq UR_k \tag{20}$$

where k (k = 1, 2, . . ., K) represents the CHP units and i (i = 1,2, . . .,I_k) represents the boilers within the CHP units. q indicates BFG, COG, and coal. f_{kt} denotes the power output of the CHP unit k during time period t, and S_{krt} represents the flow rate of grade r steam produced by CHP unit k during time period t. $S_{kr}^{\min}$ and $S_{kr}^{\max}$ represent minimum and maximum allowable generation rate of the r level of steam from the CHP unit, respectively. $f_k^{\min}$ and $f_k^{\max}$ represent minimum and maximum allowable electricity generation rate from the CHP unit, respectively. DR_k and UR_k represent the maximum ramp down and up rate of the CHP unit, respectively.

(3) CDQ

The iron and steel enterprise in this study use CDQ technology to recycle waste heat in the production process. The model for the CDQ is as follows [38].

$$f_{mt} \cdot \tau_t + \sum_{r=1}^{R} (S_{mrt} \cdot \tau_t \cdot h_r^s - S_{mrt} \cdot \tau_t \cdot h^w) = \eta_m \cdot E_{mt}^{in} \tag{21}$$

$$S_{mr}^{\min} \leq S_{mrt} \leq S_{mr}^{\max} \tag{22}$$

$$f_m^{\min} \leq f_{mt} \leq f_m^{\max} \tag{23}$$

$$DR_m \leq f_{mt} - f_{mt-1} \leq UR_m \tag{24}$$

where m (m = 1, 2, . . ., M) represents the CDQ units. f_{mt} denotes the power generation of the CDQ units in time period t. S_{mrt} represents the steam generation rate of the CDQ units in time period t and at level r, and E_{mt}^{in} represents the total waste heat recovered by the CDQ units in time period t. $S_{mr}^{\min}$ and $S_{mr}^{\max}$ represent the minimum and maximum allowable generation rate of the r level of steam from the waste heat unit, respectively. $f_m^{\min}$ and $f_m^{\max}$ represent the minimum and electricity generation rate from the waste heat unit, respectively. DR_m and UR_m represent the maximum ramp down and up rate of the waste heat unit, respectively.

B. Gas, Steam, and Power Balances

In terms of power balance, the generator units comprise steam turbine units, CHP units, and waste heat recovery units. The total power generation of the generator units must meet the electricity consumption of the production process in each time period. The power balance equation is [31]

$$\sum_{j=1}^{j} f_{jt} + \sum_{k=1}^{k} f_{kt} + \sum_{m=1}^{M} f_{mt} + f_t^{imp} = f_t^{dem} + f_t^{\exp} \tag{25}$$

$$y_t^{\mathrm{imp}} + y_t^{\mathrm{exp}} = 1 \tag{26}$$

$$0 \le f_t^{\mathrm{imp}} \le f_t^{\mathrm{imp,max}} \cdot y_t^{\mathrm{imp}} \ \forall t \tag{27}$$

$$0 \le f_t^{\mathrm{exp}} \le f_t^{\mathrm{exp,max}} \cdot y_t^{\mathrm{exp}} \ \forall t \tag{28}$$

where f_t^{dem} is the demand for power, f_t^{imp} is the electricity purchase from the grid in each period, and f_t^{exp} is the electricity sales of the grid during each period. y_t^{imp} and y_t^{exp} are 0–1 variables indicating the purchase and sale states, respectively. $f_t^{\mathrm{imp,max}}$ and $f_t^{\mathrm{exp,max}}$ are the maximum power purchase and sale limits during t, respectively.

The steam is generated by boilers, CHP units, and CDQ units. The steam balance equation is

$$\sum_{i}^{I} S_{irt} + \sum_{k=1}^{K} S_{krt} + \sum_{m=1}^{M} S_{mrt} + \left(\sum_{j=1}^{j} S_{jrt}^{out} - \sum_{j=1}^{j} S_{jrt}^{\mathrm{in}} \right) = S_{rt}^{\mathrm{dem}} \tag{29}$$

where S_{rt}^{dem} represents the steam demand for grade r during time period t from the production process.

The gas storage of the gasholders at the end of each optimization cycle is

$$inv_{qt} = inv_{q(t-1)} + V_{qt}^{\mathrm{gen}} \cdot \tau_t - \sum_{u=1}^{U} \left(V_{qtu} \cdot \tau_t \right) - \sum_{i=1}^{I} \left(V_{iqt} \cdot \tau_t \right) - Q_{\mathrm{emission}} \tag{30}$$

where q (q = 1, 2, . . ., Q_{g}) represents different types of gases, inv_{qt} denotes the storage level of gas type q in the gas holder at the end of time period t, V_{qt}^{gen} represents the generation rate of gas type q, V_{qtu} indicates the consumption rate of gas type q in the steel production process u, V_{iqt} denotes the consumption rate of gas type q in equipment i of the energy recovery system during time period t, and Q_{emission} represents the amount of gas dissipated during time period t.

C. Gas Holder Operational Model

The gas holder, as a buffering device, can store excess gas or supply the required amount of gas to the production process, serving as a buffer. The gas storage amount in the gas holder must remain within its capacity limits, which can be expressed [39]

$$Inv_q^{\min} \le Inv_{qt} \le Inv_q^{\max} \ \forall q \in \mathbf{Q}_x, t \tag{31}$$

where $Inv_q^{\min}$ and $Inv_q^{\max}$ represent the minimum and maximum capacity of gas holders, respectively.

In addition to the capacity limits, the gas storage volume of the gas holders should remain within a safe operating range to provide standby gas for the production process. Otherwise, operational risks may arise. This constraint can be expressed as

$$Inv_q^{\mathrm{L}} - SInv_{qt}^{\mathrm{L}} \le inv_{qt} \le Inv_q^{\mathrm{H}} + SInv_{qt}^{\mathrm{H}} \ \forall q \in \mathbf{Q}_x, t \tag{32}$$

where Inv_q^{H} and Inv_q^{L} represent the high and low boundaries of the gas storage safety operation range, respectively. $SInv_{qt}^{\mathrm{L}}$ and $SInv_{qt}^{\mathrm{H}}$ are two positive slack variables used to represent the deviation of the gas holder's storage level from the safety operation range. Through optimization, the gas holder's storage level can be controlled to minimize system operating costs while ensuring production safety.

D. Burner Operational Constraints

Industrial boilers in steel plants are typically equipped with multiple identical burners used to introduce different types of gas. By controlling the opening and closing of burners, the gas intake can be adjusted. However, frequently opening and closing burners may lead to backfiring or incomplete combustion. Therefore, to maintain the stability of the combustion process in the boiler, the number of burner switches should be minimized. In the actual operation, a maximum of three burner state changes are allowed per time period. The total amount of gas entering the boiler during each time period is [32]

$$V_{iqt} = V_{iq} \cdot N_{iqt} \ \forall q \in \mathbf{Q}_x, t \tag{33}$$

where N_{iqt} represents the number of burners that are in the "on" state during time period t. V_{iq} denotes the consumption rate of gas type q in each burner of the energy recovery system equipment i.

Define ΔN_{iqt} as the number of burners whose on/off status changes during time period t. The constraint equations for ΔN_{iqt} are

$$\Delta N_{iqt} \geq N_{iqt} - N_{iq(t-1)} \ \forall q \in \mathbf{Q}_x, t \tag{34}$$

$$\Delta N_{iqt} \geq N_{iq(t-1)} - N_{iqt} \ \forall q \in \mathbf{Q}_x, t \tag{35}$$

$$\Delta N_{iqt} = ibn^1_{iqt} + ibn^2_{iqt} + ibn^3_{iqt} \ \forall q \in \mathbf{Q}_x, t \tag{36}$$

where ibn^1_{iqt}, ibn^2_{iqt}, and ibn^3_{iqt} are binary variables, representing the cases where the status of 1, 2, and 3 burners changes, respectively.

E. Objective Function

The objective function is to minimize the operational cost of the GSPS coupled system considering the TOU tariff:

$$Y = y^{\text{coal}} + y^{\text{ele}} + y^{\text{p1}} + y^{\text{p2}} + y^{\text{p3}} + y^{\text{p4}} + y^{\text{main}} \tag{37}$$

$$y^{\text{coal}} = \sum_{t=1}^{T} \sum_{k=1}^{K} (C_q \cdot V_{iqt} \cdot \tau_t) q = \text{coal} \tag{38}$$

where C_q is the price of the coal and y^{coal} is the purchasing coal cost,

$$y^{\text{ele}} = \sum_{t=1}^{T} \left(C_t^{\text{exp}} \times f_t^{\text{exp}} \times \tau_t \right) - \sum_{t=1}^{T} \left(C_t^{\text{imp}} \times f_t^{\text{imp}} \times \tau_{\text{t}} \right) \tag{39}$$

where C_t^{exp} is the electricity sale price in period t, C_t^{imp} is the electricity purchase price in period t and y^{ele} is the cost of purchasing/selling electricity from the grid,

$$y^{\text{p1}} = \sum_{t=1}^{T} \left(E_q^{em} \cdot Q_{qt}^{em} \right) \tag{40}$$

where E_q^{em} is the penalty coefficient for gas emission of the q type of the byproduct gas and y^{p1} is punished by the gas dispersion,

$$y^{\text{p2}} = \sum_{t=1}^{T} \left(E_q^{\text{L}} \cdot SInv_{qt}^{\text{L}} + E_q^{\text{H}} \cdot SInv_{qt}^{\text{H}} \right) \tag{41}$$

where E_q^L is the penalty coefficient for the inventory level in gasholder q which lies in its low operational region, E_q^H is the penalty coefficient for the inventory level in gasholder q which lies in its high operational region and y^{p2} is the penalty cost of the gasholder cabinet,

$$y^{\text{p3}} = \sum_{t=1}^{T} \sum_{i=1}^{I} \left[E_q^{SW} \times \left(ibn^1_{iqt} + ibn^2_{iqt} + ibn^3_{iqt} \right) \right] \tag{42}$$

where E_q^{SW} is the penalty coefficient for burner switching operations for the q type of byproduct gas and y^{p3} is the penalty cost of the boiler burner switch

$$y^{\text{p4}} = \sum_{t=1}^{T} \sum_{i=1}^{I} \left[E_q^{2S} \times ibn_{iqt}^2 + E_q^{3S} \times ibn_{iqt}^3 \right] \tag{43}$$

where E_q^{2W} is the penalty coefficient for simultaneously switching two burners related to the q type of byproduct gas in a boiler, E_q^{3W} is thepenalty coefficient for simultaneously switching three burners related to the q type of byproduct gas in a boiler, and y^{p4} is the additional penalty cost for simultaneous switches of burners in fuel boilers,

$$\begin{aligned} y^{\text{main}} = \sum_{t=1}^{T} \sum_{i=1}^{I} (C_i^m \times S_{it} \times \tau_t) + \sum_{t=1}^{T} \sum_{j=1}^{J} \left(C_j^{PM} \times f_{jt} \times \tau_t \right) + \\ \sum_{t=1}^{T} \sum_{k=1}^{K} (C_k^{PM} \times f_{kt} \times \tau_t) + \sum_{t=1}^{T} \sum_{m=1}^{M} (C_m^{PM} \times f_{mt} \times \tau_t) \end{aligned} \tag{44}$$

where C_i^m is the maintenance cost of boiler i, C_j^{PM} is the maintenance cost of turbine j, C_k^{PM} is the maintenance cost of CHP unit k, C_k^{PM} is the maintenance cost of waste heat and unit m, and y^{main} is the equipment maintenance costs.

4. Case Study

Taking the industrial production of a steel plant in Northeast China as an example, this study optimizes the operation strategy of the GSPS in response to the TOU tariff, while ensuring the steel production requirements. The GSPS consists of four boilers, two CHP units, and two CDQ units, with the system schematic depicted in Figure 1. The steel plant's production schedule for the entire day is shown in Figure 2. Figure 2a illustrates the by-product gas and waste heat production for each time period in the main steel production processes. Since CDQ2 requires supplementary S2 steam, the amount of waste heat required is higher than for CDQ1. Due to the intermittent nature of the converter process, LDG is fully utilized for the blast furnace and hot rolling processes and is not included in the optimization scheduling. Figure 2b displays the demand for BFG, COG, and various grades of steam in the steel production process. Parameters for boilers, turbines, CHP units, etc. are given in the Appendix A.

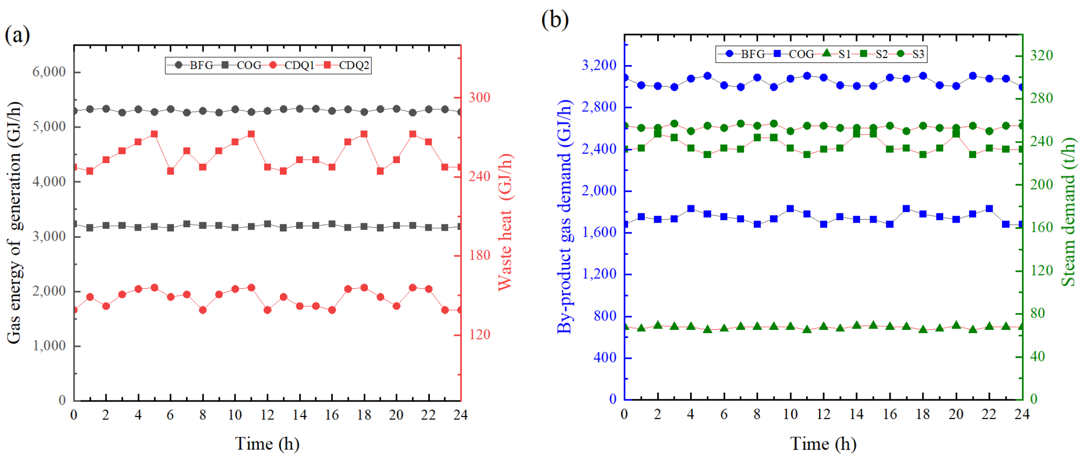

Figure 2. (**a**) energy generation; (**b**) energy demand.

The TOU electricity pricing for a typical steel enterprise is presented in Table 1 [40], where 08:00–12:00 and 19:00–23:00 are the peak prices, with the price of 0.7188 ¥/kWh, 12:00–19:00 is the moderate price by 0.4917 ¥/kWh, and 23:00–08:00 is the valley price by 0.2796 ¥/kWh. Traditional steel enterprises purchase electricity at contract prices, overlooking the impact of TOU tariffs on production costs following electricity market reforms, which hinders their ability to adapt to market mechanisms.

Table 1. TOU electricity price in a typical steel plant.

	Peak Price	Moderate Price	Valley Price
Time interval	08:00–12:00 19:00–23:00	12:00–19:00	23:00–08:00
Price (¥/kWh)	0.7188	0.4917	0.2796

5. Results and Discussions

Figure 3 depicts the optimized S1 steam generation in each period. S1 steam is generated in boilers B1-B4 from the by-product gases BFG and COG. Since the S1 steam needs to meet the main steel production process demand for various types of steam, it is always in full production. The by-product gas introduced in B3 and B4 is all BFG, and its capacity is greater than that of B1 and B2. Notably, the S1 steam required for the production process is primarily supplied by B1 and B2, with the remaining demand met by the supplementary contributions from B3 and B4. The surplus S1 steam produced by B3 and B4 serves as thermal energy for the generation of electricity by TB1, TB2, and the generation of S2 and S3 steam.

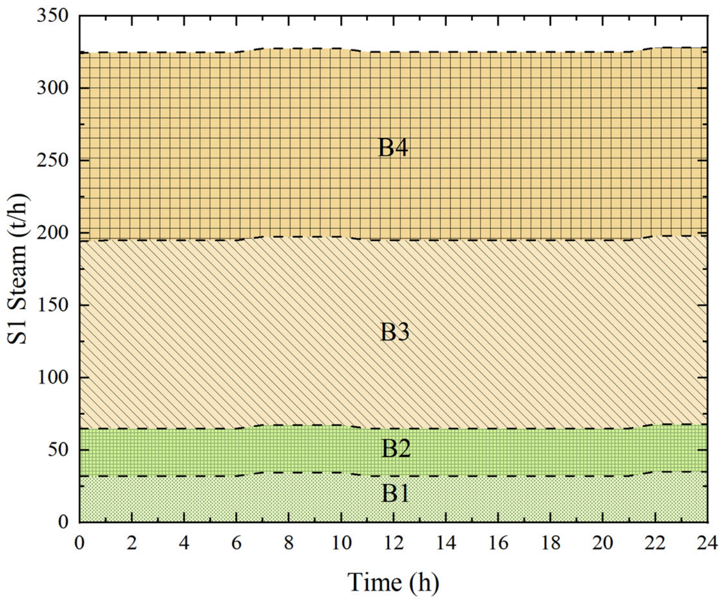

Figure 3. Steam generation in various boilers.

Figure 4 illustrates the output of S2 steam in various devices in each time period, where S2 steam is generated by TB1, TB2, CHP1, CHP2, and CDQ2. Considering the impact of the TOU tariff, the electricity demand in the steel production process is mainly met by the grid during the valley hours (23:00–08:00). On the contrary, the coal usage for CHP units needs to be increased during the moderate and peak hours. Since the operating efficiency of CHP1 is lower than that of CHP2, priority should be given to adjusting the coal purchase of CHP1 according to the TOU tariff. Meanwhile, the S2 steam produced by CHP1 adjusts according to the TOU tariff. To ensure the steel production demand, the S2 steam produced by TB1 and TB2 changes with the CHP1 adjustment strategy, while the CHP2 and CDQ units remain at full-load operation. Considering the efficiency differences between the two CDQ units in practical operation, the more efficient CDQ2 unit is prioritized when steam generation is required. Furthermore, since the CDQ2 unit has not reached its maximum adjustable capacity, the less efficient CDQ1 unit is not adjusted for use.

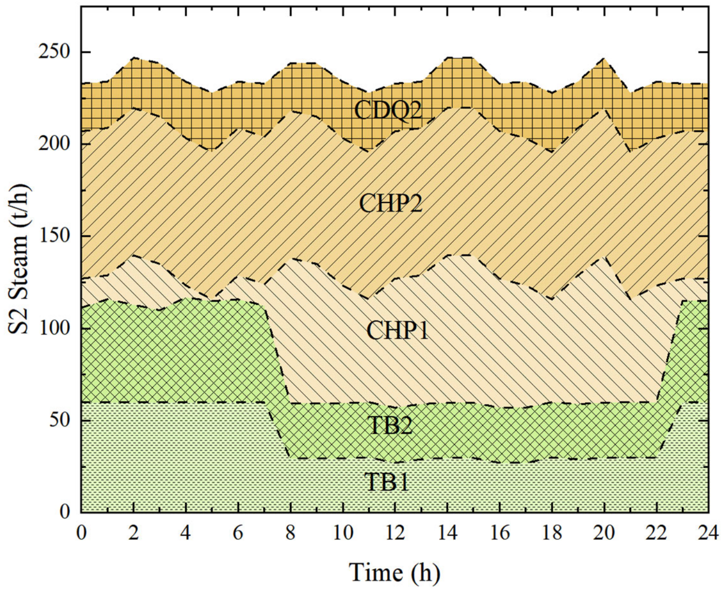

Figure 4. S2 Steam generation at TOU tariff.

Figure 5 depicts the S3 steam output in various devices in each time period. S3 steam is produced by TB1, TB2, and CHP2. Since the S2 steam increases with the rise in power generation in CHP1 during the moderate and peak hours, the S2 steam produced by TB1 and TB2 decreases, resulting in an increase in the S3 steam. To meet the requirement of S3 steam in the production process, S3 steam produced by CHP2 decreases accordingly. In the valley hours, the S3 steam presents an opposite trend to moderate and peak hours.

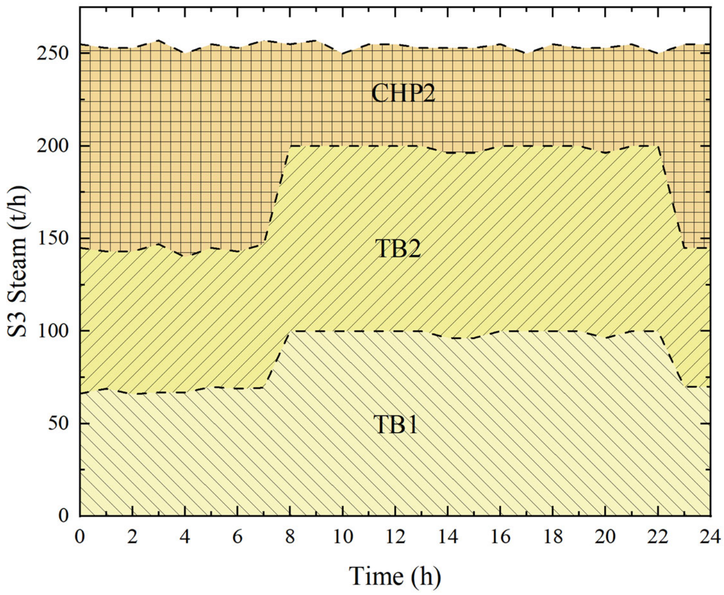

Figure 5. S3 Steam generation at TOU tariff.

Figure 6 depicts the electricity generation and purchase during 24 h considering the TOU tariff. Since there is no power generation cost from by-product gases, the TB, CHP, and CDQ in the GSPS are at full capacity under NTOU states. At this time, the remaining electricity required in the steel production process is provided by the grid. Self-generated electricity accounts for 64.4% of the total power load. Under the implementation of the

TOU tariff mechanism, the electricity generation in the GSPS during the valley price period (23:00 to 08:00) decreases significantly due to the lower electricity purchase cost. Meanwhile, the coal consumption in the CHP units during this time period decreases by 406.3 tons, as shown in Figure 7. On the contrary, the power generation of the GSPS at full capacity during the peak and moderate price period. If the steel enterprise is considered as a virtual power plant, its power regulation capacity when participating in the TOU tariff mechanism accounts for approximately 26.94% of the NTOU tariff. The results show that by participating in the TOU tariff mechanism, the GSPS can fully utilize the load regulation potential of steel enterprises, thereby enhancing the adaptability and flexibility of their electricity consumption behavior.

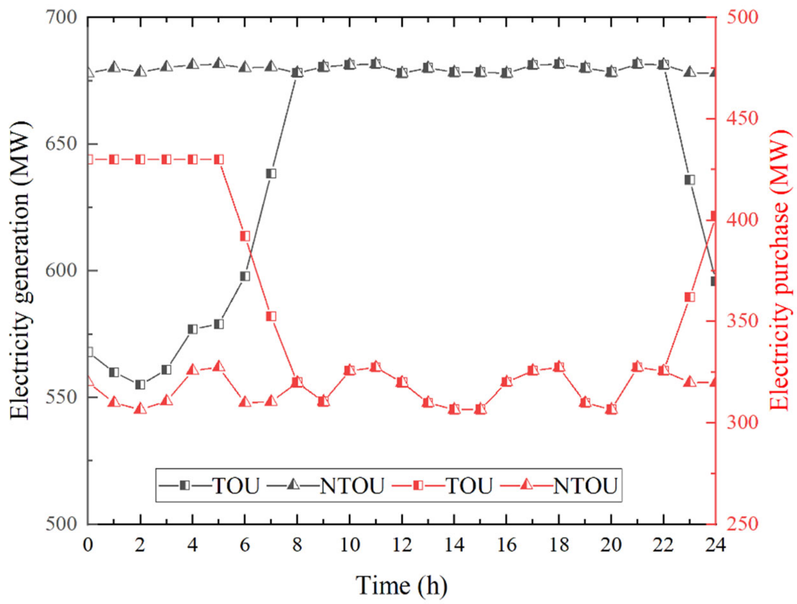

Figure 6. Electricity generation and purchase during various time periods.

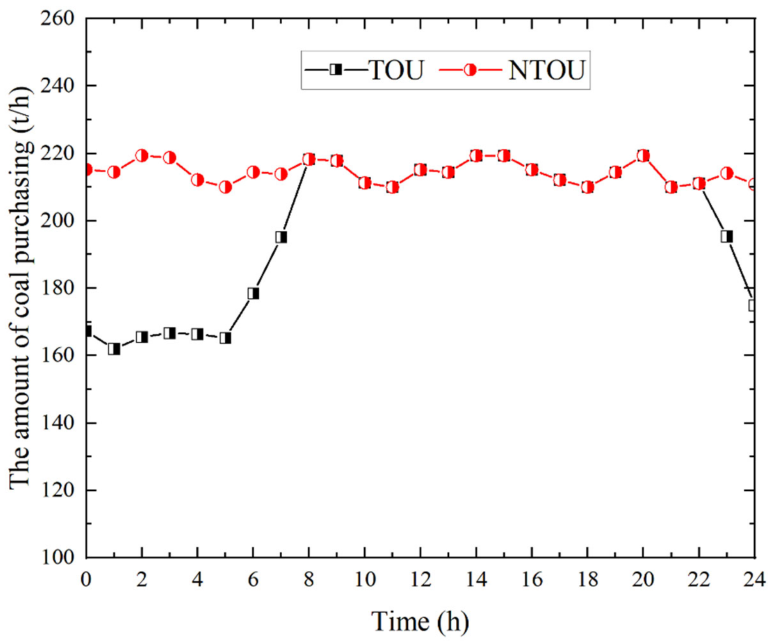

Figure 7. Coal purchase during various time periods.

Figure 8 illustrates the electricity and coal purchase costs for the steel enterprise at different times of day. After the implementation of the TOU tariff mechanism, the coal consumption of CHP units during the valley price hours is reduced, resulting in a decrease in the cost of purchased coal. The peak of the power purchase is actually from 0:00 to 7:00 p.m., during which the amount of power purchased increases, but the cost of the power purchase decreases due to the low price of electricity at this time. Overall, the cost of energy (including electricity and coal prices) is reduced by 2.24% after the GSPS optimized dispatch under the TOU tariff mechanism.

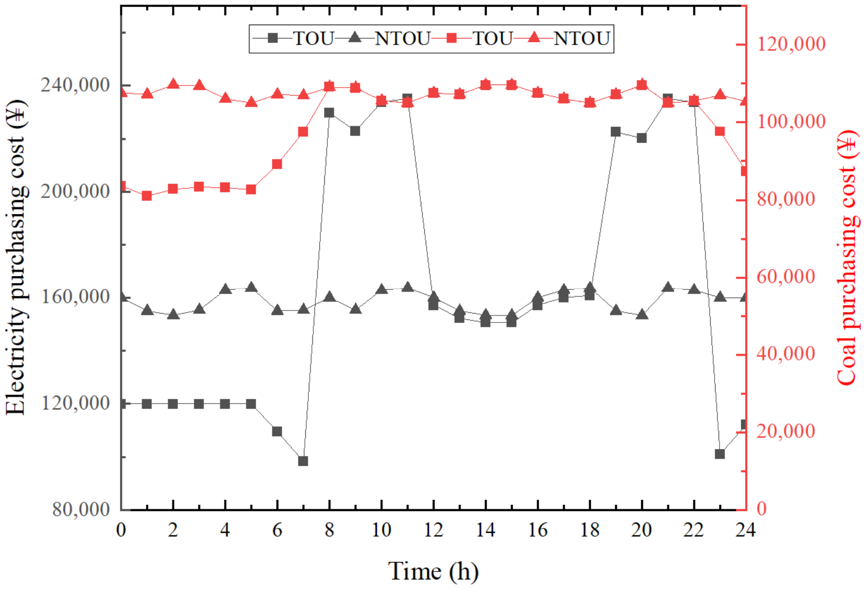

Figure 8. Electricity and coal purchase costs for the steel enterprise.

Based on the above study, this paper further analyzes the impact of coal prices on electricity generation and purchase in the GSPS. For the coal prices of 0.3 ¥/kg, 0.7 ¥/kg, and 1 ¥/kg, the optimization and scheduling results are shown in Figure 9. In Figure 9a, when the coal price is 0.3 ¥/kg, due to the low cost of power generation, the electricity production and purchase of the GSPS have always been at the upper and lower limits, respectively. In Figure 9b, due to the steam demands of production processes, the GSPS must operate a certain number of units for power generation and cannot fully rely on purchased electricity. When the coal price increases, the electricity demands for the steel production primarily rely on the steam power generation and grid, which leads to a decrease in coal purchases and an increase in electricity purchases, especially in the valley price period. When the coal price is 1¥/kg, purchasing coal for power generation is best avoided. Therefore, the changing trends in electricity generation and purchase are similar to that of the TOU tariff.

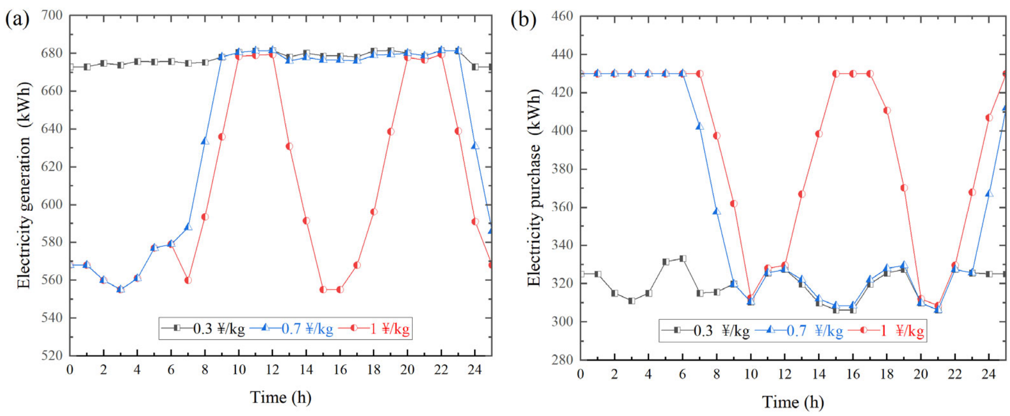

Figure 9. Electricity generation and purchase at different coal prices.

In general, the model successfully adjusts generation levels according to the TOU tariff, maintaining the general trend of "more self-generation during high electricity price periods and more electricity purchasing during low price periods". This demonstrates that the proposed optimization scheduling model effectively identifies the most reasonable power production strategy under varying coal price conditions, highlighting its robustness and effectiveness.

6. Conclusions

This study investigates the optimal energy scheduling strategy for the GSPS in steel enterprises, taking into account the TOU tariff mechanism. The model integrates various forms of energy such as electricity, heat, and gas, as well as various items of energy conversion and transmission equipment, such as boilers, steam turbines, CHP units, and CDQ units. Based on the MILP method, an innovative GSPS optimization model is developed to solve the distribution strategy of various energies during the dispatching period, while ensuring energy supply stability and production safety. The results show that after participating in the TOU tariff mechanism, more efficient CHP units play a central role in demand response. The GSPS adjusts the relationship between coal, steam power generation, and purchased electricity according to the TOU tariff in the dispatching period to reduce the energy costs. Specifically, by increasing the amount of purchased electricity and reducing coal consumption during the valley price period, a 2.24% reduction in GSPS energy costs was achieved.

In contrast to previous studies, this study added the burner switching problem with TOU tariffs. Firstly, the burner switching problem involving fuel boilers in actual production is considered. In actual production, the change in the fuel flow rate needs to be controlled by the burner switch, and the switch is affected by the safety of production and cannot be changed arbitrarily. Most importantly, we added TOU tariffs to the energy system model, which provides a more flexible way of using electricity in steel mills.

Under the influence of the TOU tariff mechanism, the load regulation capability of the steel enterprise increased by 26.94%. Meanwhile, the load regulation strategy is also affected by coal prices. By optimizing the secondary energy allocation within the steel enterprises, this study not only reduces the overall energy cost, but also enhances the flexibility of the demand response, providing theoretical support for the integration of renewable energy in steel enterprises. This research provides an important theoretical basis for optimizing energy scheduling, reducing costs, and enhancing flexibility in steel enterprises, with positive implications for promoting their participation in sustainable energy market development.

Author Contributions: Methodology, Y.J. and H.M.; Software, Y.Z.; Investigation, Y.J.; Resources, Q.H.; Data curation, Y.Z. and Q.H.; Writing—original draft, J.Y.; Writing—review & editing, N.M.; Visualization, M.Z.; Supervision, N.M. All authors have read and agreed to the published version of the manuscript.

Funding: This work is supported by the State Grid Corporation of China Headquarters Management of Science and Technology Project (5400-202328576A-3-2-ZN).

Data Availability Statement: Dataset available on request from the authors. The raw data supporting the conclusions of this article will be made available by the authors on request.

Conflicts of Interest: Authors Jun Yan, Qianpeng Hao and Minhao Zhang were employed by the company Inner Mongolia Power (Group) Co., Ltd. The remaining authors declare that the research was conducted in the absence of any commercial or financial relationships that could be construed as a potential conflict of interest.

Nomenclature

t	period
R	steam
J	steam turbine
K	CHP unit
M	CDQ unit
Q_g	different types of gases
S_{irt}	flow rate of steam, ton/h
S_{it}^{w}	feedwater flow rate of boiler, ton/h
V_{iqt}	feed flow rate of fuel q, km^3/h
η	thermal efficiency of boiler
hv_q	heating value of fuels
h	enthalpy
S_{jt}	steam flow of the steam turbine, ton/h
S_{jrt}	flow of grade r steam of the steam turbine, ton/h
$f_{j,t}$	power generation of steam turbine, MW/h
f_{kt}	power output of CHP, MW/h
S_{krt}	flow rate of steam, ton/h
f_{mt}	power generation of the CDQ, MW/h
E_{in}^{mt}	total waste heat recovered by the CDQ, GJ/h
f_t^{dem}	demand for power, MW
f_t^{imp}	electricity purchase, MW
f_t^{exp}	electricity sales, MW
S_{rt}^{dem}	steam demand, km^3
y	costs
V_{qt}^{gen}	generation rate of gas, km^3/h
V_{qtu}	consumption rate of gas, km^3/h
Q_{emission}	flaring amount of gas, km^3
DR	demand response
GSPS	gas–steam–power system
TOU	time-of-use
MILP	mixed-integer linear programming
CDQ	coke dry quenching
NTOU	not time-of-use
CHP	combined heat and power
COG	gas recovered from the coking process
BFG	gas recovered from blast furnace
LDG	gas recovered from the converter process

Appendix A

Table A1. Data for boilers.

Boiler	**Efficiency (η_i)**	$V_{ibfg}^{\max}$ **(m^3/h)**	$V_{icog}^{\max}$ **(m^3/h)**	$S_{i,HP}^{\min}$ **(t/h)**	$S_{I,HP}^{\max,}$ **(t/h)**	$hv_i^{\min}$ **(GJ/m^3)**
B1	0.89	40	6	0	35	0.0035
B2	0.92	40	6	0	35	0.0035
B3	0.84	120	7	0	130	0.0035
B4	0.86	120	7	0	130	0.0035

Table A2. Initial burner switching data in boilers and CHP units.

Boilers	Initial Number		Inlet Flow Rate per Burner (m^3/h)	
	COG	BFG	COG	BFG
B1	2	4	0.5	5
B2	2	4	0.5	5
B3	0	23	0.5	5
B4	0	23	0.5	5
CHP1	14	16	2	10
CHP2	14	16	2	10

Table A3. Gasholders capacity.

Volume	COG	BFG	LDG
Minimum capacity (m^3)	40	50	15
Low operational inventory level (m^3)	80	140	25
Normal operational inventory level (m^3)	100	180	40
High operational inventory level (m^3)	120	220	55
Maximum capacity (m^3)	135	260	70

Table A4. Calorific value of gases, coal, and natural gas, and enthalpy of boiler feedwater and steam.

	COG (GJ/m^3)	BFG (GJ/m^3)	LDG (GJ/m^3)	Coal
Calorific value	0.018	0.0035	0.0075	0.0218
Item	**Boiler feed water (GJ/kg)**	**S1 (GJ/kg)**	**S2 (GJ/kg)**	**S3 (GJ/kg)**
Enthalpy	0.00010538	0.0033	0.0031	0.00293

Table A5. Parameters such as the maximum inlet and outlet power of the plant, penalty coefficient, etc.

Parameters	Value
Maximum imported power (MW)	130
Maximum exported power (MW)	100
Penalty coefficient for gas emission (¥/m^3)	100
Penalty coefficient for violation of high operational level (¥/m^3)	10
Penalty coefficient for violation of low operational level (¥/m^3)	5
Penalty coefficient for burner switches (¥/switch)	800
Penalty coefficient for simultaneous switches of two burners (¥/instance)	100
Penalty coefficient for simultaneous switches of three burners (¥/instance)	200
Maintenance cost of boilers (¥/t)	6
Maintenance cost of turbines (¥/kWh)	0.06
Maintenance cost of CHP units (¥/kWh)	0.08
Maintenance cost of CDQ units(¥/kWh)	0.06
Coal purchase cost (¥/t)	500
Electricity sale price (¥/kWh)	0.2

Table A6. Data for steam turbine units.

TB	Efficiency (η_j)	$S_{j,HP}^{in,min}$ (t/h)	$S_{j,HP}^{in,max}$ (t/h)	$S_{j,MP}^{out,min}$ (t/h)	$S_{j,MP}^{out,max}$ (t/h)	$S_{j,LP}^{out,min}$ (t/h)	$S_{j,LP}^{out,max}$ (t/h)	f_j^{min} (MW)	f_j^{max} (MW)	DR_j (MW/h)	UR_j (MW/h)
TB1	0.82	60	130	0	60	0	100	0	25	5	5
TB2	0.85	60	130	0	60	0	100	0	25	5	5

Table A7. Data for CHP units.

CDQ	Efficiency (η_m)	$S_{m,HP}^{min}$ (t/h)	$S_{m,HP}^{max}$ (t/h)	$S_{m,LP}^{min}$ (t/h)	$S_{m,LP}^{max}$ (t/h)	f_m^{min} (MW)	f_m^{max} (MW)	DR_m (MW/h)	UR_m (MW/h)
CDQ1	0.73	0	40	0	60	0	30	5	5
CDQ2	0.75	0	40	0	60	0	30	5	5

Table A8. Data for CDQ units.

CHP	Efficiency (η_k)	$V_k^{BFG,max}$ (m^3/h)	$V_k^{COG,max}$ (m^3/h)	hv_k^{min} (GJ/m^3)	$S_{k,MP}^{min}$ (t/h)	$S_{k,MP}^{max}$ (t/h)	$S_{k,LP}^{min}$ (t/h)	$S_{k,IP}^{max}$ (t/h)	f_k^{min} (MW)	f_k^{max} (MW)	DR_k (MW/h)	UR_k (MW/h)
CHP1	0.38	0	130	0.0046	0	80	0	110	220	300	20	20
CHP2	0.39	0	130	0.0046	0	80	0	110	220	300	20	20

Table A9. Gas generation rate, steam and electricity demand, and CDQ recovery.

Period	Gases (m^3/h)			CDQ (GJ)		Power (MW)	Steam (t/h)		
	BFG	COG	LDG	CDQ1	CDQ2		S1	S2	S3
0	1514	179.50	47	138.965	247.400	698	68	233	255
1	1523	175.50	46	138.965	244.365	690	66	234	253
2	1525	177.70	45	138.965	252.940	685	69	247	253
3	1505	177.80	45	138.965	259.550	691	68	244	257
4	1522	175.70	49	138.965	266.540	707	68	234	250
5	1508	176.80	38	138.965	272.540	709	65	228	255
6	1523	175.50	47	138.965	244.367	690	66	234	253
7	1505	179.50	46	138.965	259.549	691	68	233	257
8	1514	177.80	45	138.965	247.403	698	68	244	255
9	1505	177.80	45	138.965	259.555	691	68	244	257
10	1522	175.70	49	138.965	266.537	707	68	234	250
11	1508	176.80	38	138.965	272.542	709	65	228	255
12	1514	179.50	47	138.965	247.403	698	68	233	255
13	1523	175.50	46	138.965	244.363	690	66	234	253
14	1525	177.70	45	138.965	252.937	685	69	247	253
15	1525	177.70	45	138.965	252.942	685	69	247	253
16	1514	179.50	49	138.965	247.396	698	68	233	255
17	1522	175.70	38	138.965	266.542	707	68	234	250
18	1508	176.80	47	138.965	272.536	709	65	228	255
19	1523	175.50	46	138.965	244.371	690	66	234	253
20	1525	177.70	45	138.965	252.942	685	69	247	253
21	1505	177.80	38	138.965	272.538	709	65	228	255
22	1522	175.70	38	138.965	266.543	707	68	234	250
23	1522	175.70	49	138.965	247.399	698	68	233	255
24	1508	176.80	45	138.965	247.404	698	68	233	255

References

1. Notice of the Ministry of Industry and Information Technology of the People's Republic of China on the Release of Energy Efficiency Benchmark Levels and Benchmark Levels in Key Areas of High Energy Consuming Industries (2021 Edition) by Five Departments. 15 November 2021. Available online: https://www.miit.gov.cn (accessed on 22 June 2023).
2. Shahabuddin, M.; Brooks, G.; Rhamdhani, M.A. Decarbonisation and hydrogen integration of steel industries: Recent development, challenges and technoeconomic analysis. *J. Clean. Prod.* **2023**, *395*, 136391. [CrossRef]
3. Watari, T.; McLellan, B. Global demand for green hydrogen-based steel: Insights from 28 scenarios. *Int. J. Hydrogen Energy* **2024**, *79*, 630–635. [CrossRef]
4. Zhang, J.; Shen, J.; Xu, L.; Zhang, Q. The CO_2 emission reduction path towards carbon neutrality in the Chinese steel industry: A review. *Environ. Impact Assess. Rev.* **2023**, *99*, 107017. [CrossRef]
5. Li, W.; Zhang, S.; Lu, C. Research on the driving factors and carbon emission reduction pathways of China's iron and steel industry under the vision of carbon neutrality. *J. Clean. Prod.* **2022**, *361*, 132237. [CrossRef]
6. Lin, B.; Wu, R. Designing energy policy based on dynamic change in energy and carbon dioxide emission performance of China's iron and steel industry. *J. Clean. Prod.* **2020**, *256*, 120412. [CrossRef]
7. Ren, L.; Zhou, S.; Peng, T.; Ou, X. A review of CO_2 emissions reduction technologies and low-carbon development in the iron and steel industry focusing on China. *Renew. Sustain. Energy Rev.* **2021**, *143*, 110846. [CrossRef]
8. Zhang, Q.; Di, W.; Du, T.; Cai, J. Coupling Model of Surplus Gas-Steam-Electricity and Its Application in Steel Enterprises. *CIESC J.* **2011**, *62*, 753–758.
9. Xu, T.; Huo, Z.; Wang, W.; Xie, N.; Li, L.; Liu, Y.; Mu, L. Evaluation of by-product-gas utilization options for carbon reduction at an integrated iron and steel mill. *Energy* **2024**, *294*, 130959. [CrossRef]
10. Branca, T.A.; Colla, V.; Algermissen, D.; Granbom, H.; Martini, U.; Morillon, A.; Pietruck, R.; Rosendahl, S. Reuse and recycling of by-products in the steel sector: Recent achievements paving the way to circular economy and industrial symbiosis in Europe. *Metals* **2020**, *10*, 345. [CrossRef]
11. Sui, P.; Ren, B.; Wang, J.; Wang, G.; Zuo, H.; Xue, Q. Current situation and development prospects of metallurgical by-product gas utilization in China's steel industry. *Int. J. Hydrog. Energy* **2023**, *48*, 28945–28969. [CrossRef]
12. Zhang, Q.; Zhao, X.; Lu, H.; Ni, T.; Li, Y. Waste energy recovery and energy efficiency improvement in China's iron and steel industry. *Appl. Energy* **2017**, *191*, 502–520. [CrossRef]
13. Si, M. The Feasibility of Waste Heat Recovery and Energy Efficiency Assessment in a Steel Plant. Master's Thesis, University of Manitoba, Winnipeg, MB, Canada, 2011.
14. Liu, J.; Chang, Y. Research on Models of Power Production in Integrated Iron and Steel Factory. *J. Northeast. Univ. (Nat. Sci.)* **2014**, *35*, 1719.
15. Hu, Z.; He, D. Operation scheduling optimization of gas–steam–power conversion systems in iron and steel enterprises. *Appl. Therm. Eng.* **2022**, *206*, 118121. [CrossRef]
16. Supply, T.P. Demand response potential assessment of steel plant based on refined simulation. *Methods* **2023**, *24*, 25.
17. Masebinu, R.O. Assessing the Potential for Flexible Demand-Side Management in the Steel Industrial Sector in South Africa. Master's Thesis, University of Johannesburg, Johannesburg, South Africa, 2021.
18. Yuan, Y.; Na, H.; Chen, C.; Qiu, Z.; Sun, J.; Zhang, L.; Du, T.; Yang, Y. Status, Challenges, and Prospects of Energy Efficiency Improvement Methods in Steel Production: A Multi-Perspective Review. *Energy* **2024**, *304*, 132047. [CrossRef]
19. Ming, D.; Li, J.; Yin, Y. Optimization Scheduling Model Study for Coke Oven Gas in Steel Companies. *Comput. Eng. Des.* **2008**, *6*, 1575–1578.
20. Zhang, X.; Zhang, Y.; Tang, L. Optimization Model for the Blending and Allocation of Coke Oven Gas in Steel Enterprises. *J. Syst. Eng.* **2011**, *26*, 710–717.
21. Chen, J.; Zhou, W.; Wang, H. Study on optimal multi-period operational strategy for steam power system in steel industry. *Chem. Ind. Eng. Prog.* **2017**, *36*, 1589–1596.
22. Li, J. Optimization Scheduling of the Steam System in Steel Enterprises. Master's Thesis, Tianjin University of Technology, Tianjin, China, 2016.
23. Hao, F.; Gao, Q.; Jiang, B.; Chen, G. Research and Application of Intelligent Power Dispatching Integrated System in Steel Enterprises. *Metall. Ind. Autom.* **2013**, *37*, 33–38.
24. Ma, G. Analysis and Optimization Research of Power Systems in Integrated Steel Enterprises. Master's Thesis, Northeastern University, Boston, MA, USA, 2014.
25. Akimoto, K.; Sannomiya, N.; Nishikawa, Y.; Tsuda, T. An optimal gas supply for a power plant using a mixed interger programming model. *Utomatic* **1991**, *27*, 513–518.
26. Zhao, X.; Bai, H.; Lu, X.; Shi, Q.; Han, J. A MILP model concerning the optimisation of penalty factors for the short-term distribution of byproduct gases produced in the iron and steel making process. *Appl. Energy* **2015**, *148*, 142–158. [CrossRef]

27. García García, S.; Rodríguez Montequín, V.; Morán Palacios, H.; Mones Bayo, A. A mixed integer linear programming model for the optimization of steel waste gases in cogeneration: A combined coke oven and converter gas case study. *Energies* **2020**, *13*, 3781. [CrossRef]
28. Kong, H.; Qi, E.; Li, H.; Li, G.; Zhang, X. An MILP model for optimization of byproduct gases in the integrated iron and steel plant. *Appl. Energy* **2010**, *87*, 2156–2163. [CrossRef]
29. Jiang, S.L.; Wang, M.; Bogle, I.D.L. Plant-wide byproduct gas distribution under uncertainty in iron and steel industry via quantile forecasting and robust optimization. *Appl. Energy* **2023**, *350*, 121603. [CrossRef]
30. Shu, Y. Research on the Synergy Scheduling of Coke Oven Gas, Steam, and Electricity in Steel Enterprises. Master's Thesis, Chongqing University, Chongqing, China, 2020.
31. He, D.; Lu, X.; Feng, K.; Xu, A. Coupling Optimization Scheduling of Coke Oven Gas-Steam-Electricity System in Steel Enterprises. *Steel* **2018**, *53*, 95–104.
32. He, D.; Liu, P.; Feng, K.; Xu, A. Collaborative optimization of rolling plan and energy dispatching in steel plants. *China Metall.* **2019**, *29*, 75–80.
33. Zhao, X.; Bai, H.; Shi, Q.; Lu, X.; Zhang, Z. Optimal scheduling of a byproduct gas system in a steel plant considering time-of-use electricity pricing. *Appl. Energy* **2017**, *195*, 100–113. [CrossRef]
34. Liu, S.; Xie, S.; Zhang, Q. Multi-energy synergistic optimization in steelmaking process based on energy hub concept. *Int. J. Miner. Metall. Mater.* **2021**, *28*, 1378–1386. [CrossRef]
35. Zhao, J.; Wang, W.; Sun, K.; Liu, Y. A Bayesian networks structure learning and reasoning-based byproduct gas scheduling in steel industry. *IEEE Trans. Autom. Sci. Eng.* **2013**, *11*, 1149–1154. [CrossRef]
36. Aguilar, O.; Perry, S.J.; Kim, J.K.; Smith, R. Design and optimization of flexible utility systems subject to variable conditions: Part 1: Modelling framework. *Chem. Eng. Res. Des.* **2007**, *85*, 1136–1148. [CrossRef]
37. Mitra, S.; Sun, L.; Grossmann, I.E. Optimal scheduling of industrial combined heat and power plants under time-sensitive electricity prices. *Energy* **2013**, *54*, 194–211. [CrossRef]
38. Bischi, A.; Taccari, L.; Martelli, E.; Amaldi, E.; Manzolini, G.; Silva, P.; Campanari, S.; Macchi, E. A detailed MILP optimization model for combined cooling, heat and power system operation planning. *Energy* **2014**, *74*, 12–26. [CrossRef]
39. Zeng, Y.; Xiao, X.; Li, J.; Sun, L.; Floudas, C.A.; Li, H. A novel multi-period mixed-integer linear optimization model for optimal distribution of byproduct gases, steam and power in an iron and steel plant. *Energy* **2018**, *143*, 881–899. [CrossRef]
40. Zeng, Y.; Sun, Y. Short-Term Scheduling of Steam Power System in the Iron and Steel Industry under Time-of-Use Power Price. *J. Iron Steel Res. Int.* **2015**, *22*, 795–803. [CrossRef]